Quantitative lattice measurement of thin Langmuir-Blodgett films by atomic-force microscopy

D. K. Schwartz, J. Garnaes, R. Viswanathan, S. Chiruvolu, and J. A. N. Zasadzinski
Department of Chemical and Nuclear Engineering, University of California, Santa Barbara, California 93106
(Received 22 June 1992)

We have quantitatively determined the nature of the surface order of the outermost layer of monolayer and multilayer Langmuir-Blodgett films of cadmium arachidate, in air and under water, using atomic-force microscopy. Molecular-resolution images of 1200-nm^2 areas show that the alkyl chains of 2–5-layer films have a noncentered rectangular lattice with lattice constants of 0.482 ± 0.004 and 0.748 ± 0.006 nm, in good agreement with diffraction measurements of bulk aliphatic systems. We show unambiguously that the unit cell consists of two molecules. In contrast with the highly ordered multilayers, monolayer films have a disordered surface. Images taken under water of the head-group surface show that the bilayer surface is disordered, while thicker films show order of the alkyl chains. The presence of an underlying head-group–head-group interface with its associated cadmium ion bridging is shown to be the critical feature needed to obtain a stable and ordered surface layer.

PACS number(s): 61.16.Ch, 61.50.Jr, 61.72.Ff, 68.35.Bs

INTRODUCTION

Langmuir-Blodgett (LB) films have many applications in the areas of electronics, non-linear optics, cell membrane models, and biosensors [1]. Most of the potential applications of LB films are based on the premise of perfect molecular layering and orientation. There is also the general, but experimentally unsupported belief that the structure of the monolayer at the air-water interface is uniquely related to the structure of both monolayers and multilayers on a substrate. Hence studies of the degree and type of order of these molecularly layered films are of critical importance. In addition, LB films are model systems for the crossover between two and three dimensions and may demonstrate aspects of the physics of two dimensions including hexatic phases. Ordering in LB films has been studied by several techniques, including electron diffraction [2–5], x-ray diffraction [6,7], reflectivity [8–10], and fluorescence [11], near-edge x-ray adsorbtion fine structure (NEXAFS) [12], the surface force apparatus [13], and various spectroscopies [14–16]. These experiments have given information about molecular order and orientation averaged over areas from square micrometers to square millimeters, and typically, averaged over all of the layers of the LB film. In most of these studies and in many applications, cadmium arachidate is chosen as the prototypical material for LB films.

Recently, scanning probe microscopies, i.e., atomic-force microscopy and scanning tunneling microscopy (AFM and STM), have been used to image LB films with molecular resolution [17,18] and have been shown to be able to identify local defects and inhomogeneities in ordered surfaces [19]. The scanning tunneling microscope has been applied to structural studies of organic molecules either adsorbed or deposited on substrates, but the technique is limited to conductive substrates and layers less than a few nanometers thick, so it is of limited use for studies of LB monolayers and cannot be used for multilayers [18]. The AFM, however, is ideally suited for studies of LB films and other organic surfaces and can routinely achieve molecular resolution [17,19,20]. In addition, the AFM is extremely surface sensitive, probing only the atoms located directly at the interface with lateral resolution <1 Å, whereas other techniques measure all layers of the film with relatively poor lateral resolution. In addition, the AFM is able to image surfaces under liquids, allowing us to examine LB films with molecular resolution in air and under water [20].

Although little quantitative work has been done with the AFM, we show in this paper that, with proper attention to experimental details, lattice parameters can be measured with reproducibility and overall precision of $\sim1\%$. Difficulties that must be overcome include damage to the sample by the AFM tip, image drift due to thermal variations and hysteresis of the piezoelectric scanners, and both gross and subtle variations between AFM tips. Primarily, however, most difficulties in quantitative measurements with the AFM have stemmed from the lack of a systematic and careful calibration and imaging scheme. In addition, good-quality images of the LB film lattice must be obtained over large areas in order to determine lattice parameters with precision. We have systematically explored errors due to variations between samples and different AFM tips to minimize errors associated with imaging itself. In addition, we have obtained molecular-resolution images of LB films over areas at least ten times as large as previous results [17,19,20]. This allows us to determine the lattice symmetry and repeat distance with precision equivalents to high-resolution x-ray diffraction [7].

Although it is generally accepted that the bulk structure of thick LB films (>20 layers) of cadmium fatty acid salts is similar to that of the bulk crystal, there has been disagreement about the structure of very thin films (<10 layers) and the nature of the ordering of the layers at the air and substrate interfaces. There have been claims that the structure of the film evolves gradually toward that of a thick film as the number of layers increases from 1 to 11

[2], and that a certain number of buffer layers are necessary to eliminate the effects of the substrate on the layer ordering [15]. It has also been claimed that the outermost layer is always disordered relative to internal layers [10]. In addition, electron diffraction [2,4] and Fourier-transform infrared (FTIR) spectroscopy [16] have shown that a monolayer film has a different structure than thicker films. To resolve these questions, we have systematically studied thin films of cadmium arachidate in air and under water to determine how order evolves as the number of layers increases. Our images show that after a certain number of layers (one or two, depending on whether the substrate is hydrophobic or hydrophilic), the disordered surface of the monolayer in air or the bilayer under water gives way to the crystalline lattice of the bulk film, simply by the addition of one layer. The essential factor in determining order *in the alkyl chains* is the presence of an underlying head-group–head-group interface stabilized by cadmium ions. The primary effect of the substrate is to disallow the head-group–head-group interface, leading to the disordered monolayer or bilayer. Our results also show that the structure and phase of the monolayer on the subphase are not simply related to the structure and phase of the deposited Langmuir-Blodgett film.

EXPERIMENT

Arachidic acid [$CH_3(CH_2)_{18}COOH$, Aldrich 99%] was spread from chloroform (Fisher spectroanalyzed) solution (1.85 mg/ml) onto an aqueous (water from a Milli-Q[21] system was used) subphase in a commercial NIMA [22] trough. The subphase water included $5\times10^{-4}M$ $CdCl_2$ (Aldrich 99.99%) and was adjusted to a pH of 6.5 by addition of $NaHCO_3$ (Aldrich 99.95%). Hydrophilic substrates were freshly cleaved mica or polished silicon wafers [23] [orientation (100), 3 Ω cm, *n* type] with a rms roughness of approximately 3 Å as measured by AFM. Prior to deposition, the silicon wafers were cleaned in a hot solution of H_2O_2-H_2SO_4 (3:7 vol:vol ratio) to remove any organic contaminants while leaving the amorphous native oxide intact, then stored in clean water until use. Hydrophobic substrates were prepared by following the acid cleaning with a 5-s etch in 10% HF immediately before LB deposition, which stripped off the native oxide and left a hydrogenated and hydrophobic surface. The mica substrates were cleaned by continuous rinsing with ethanol for 5 min. After removal from the ethanol bath, the mica was cleaved using ordinary adhesive tape, and inserted into the subphase. Since all films were *Y* type (i.e., adjacent layers stack head to head or tail to tail), films deposited on a hydrophilic substrate and imaged in air had an odd number of layers (one, three, or five) while films deposited on a hydrophobic substrate and imaged in air had an even number of layers (two or four); i.e., with the methyl end of the alkyl chain at the interface. Films with an even number of layers deposited on hydrophilic substrates were transferred from the LB trough to the AFM while continuously immersed in the subphase and then imaged under water. For these films, the polar end of the arachidic acid was exposed at the interface. Isotherms and film deposition were done on the NIMA [22] trough at 22.0±0.5 °C and a surface pressure of $\pi=30\pm0.1$ dyn/cm. Film transfer was accomplished by vertical dipping at a speed of approximately 1.6 mm/min. Transfer ratios were approximately unity. Films to be imaged in air (methyl end exposed) were stored in closed containers for times ranging between one and 30 days before imaging. The length of time between deposition and imaging did not affect the images. Films to be imaged under water (polar end exposed) were examined immediately after deposition, except where noted.

AFM measurements were performed with a Nanoscope II [24] FM in air and under aqueous subphase at room temperature, using a 1×1 μm^2 scan head and a silicon nitride tip on a cantilever with a spring constant of 0.12 N/m. The best molecular resolution was achieved by using the so-called "force mode," i.e., scanning the tip at approximately constant height and measuring spring deflection. Typical repulsive forces used were on the order of 10 nN. The degree of drift in the image was evaluated by comparing Fourier transforms of images scanned in opposite directions (up and down). The initial variations between spot positions from up and down scans were often as large as 0.03 nm in amplitude and 3° in angle. However, after scanning times on a single area ranging from 0.5 to 2 h, Fourier spots from the two scan directions were in the same location within our ability to measure them given the digitization of the data on the display (0.01 nm, 0.8°). There was no damage done to the sample even after hours of continuous imaging in the AFM.

In order to calibrate the *x* and *y* (lateral) dimensions, six images of areas from 30 to 40 nm on a side were obtained from different regions (within 100 nm of each other) on a mica surface. This procedure was repeated with six different AFM tips. For each tip, the reciprocal lattice vectors (RLV) $\mathbf{b}_n$, determined from Fourier transforms, were averaged to reduce statistical fluctuations. The resulting wave vectors were parametrized by their

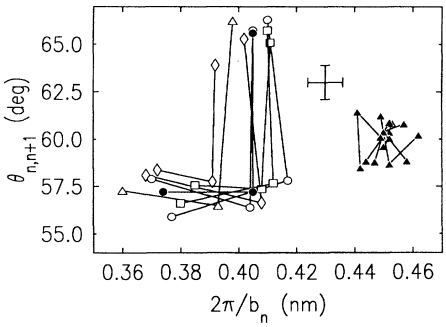

FIG. 1. Positions of Fourier spots for LB films and mica. The *x* axis corresponds to the distance between rows of molecules. The *y* axis is the angle between the given Fourier spot and the next spot in a counterclockwise direction. The various symbols refer to the following: ◇, two layers; □, three layers; △, four layers; ○, five layers; ●, best fit; ▲, mica. The error bars displayed are typical. Symbols connected by lines refer to the same sample.

magnitude, $|\mathbf{b}_n| = b_n$, and the angle between adjacent RLV's, $\theta_{n,n+1}$. The six data sets were fit to find the best overall linear calibration constants in x and y directions. The results are shown by the filled triangles in Fig. 1 which plots $\theta_{n,n+1}$ versus the lattice row repeat distance $d_n = 2\pi/b_n$. The standard deviations from the expected values for mica of $\theta_{n,n+1} = 60°$ and $b_n = 0.450$ nm (adjusted with the best-fit calibration), were $\sigma_\theta = 0.9°$ and $\sigma_b = 0.005$ nm. These numbers gave us a guideline as to the degree of reproducibility we could expect from tip to tip on the LB films. It also allowed us to estimate the absolute precision of our m independent calibrations to be $\sigma_b/m^{1/2}b_n = 0.005/\sqrt{6}\,0.450) \approx 0.5\%$.

RESULTS

Molecular-resolution images were obtained on five LB films of cadmium arachidate; two films of two layers and one film each of three, four, and five layers. Data were taken with two different AFM tips on the three- and five-layer cadmium arachidate films. A typical image and Fourier transform are shown in Fig. 2 [20]. Note that the image in Fig. 2(a) is a portion of the 30×30 nm^2 image used to obtain the Fourier transform in Fig. 2(b) and is unprocessed in any way; the detail in the larger image would be difficult to see in a journal format. This is typical of the quality of the images used to obtain lattice pa-

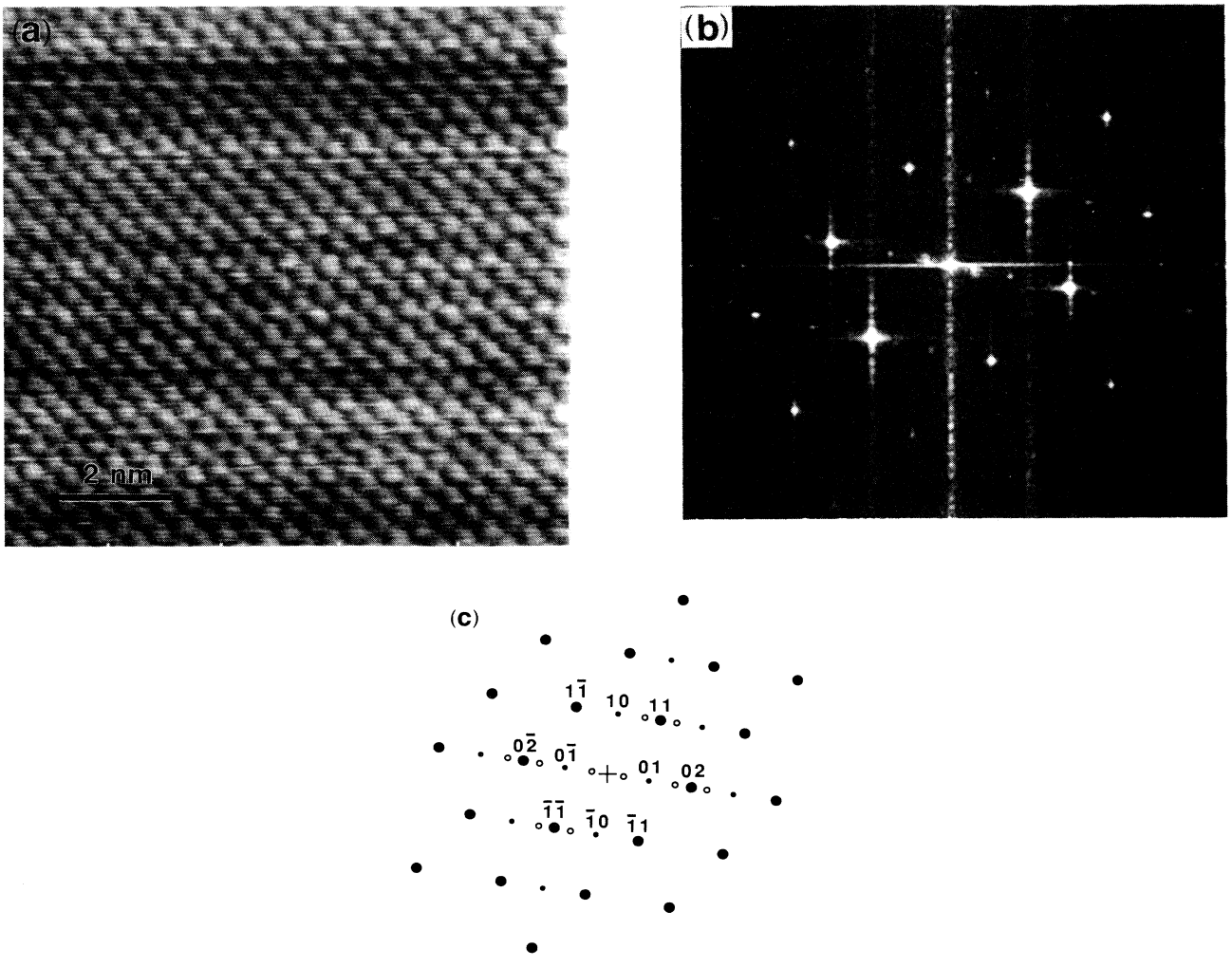

FIG. 2. (a) Raw image of a four-layer LB film of cadmium arachidate on hydrophobic silicon (10×10 nm^2). The images used for analysis were typically 35 nm on a side; however, the molecular details are easier to see in a portion cut from these images. The peak to valley height modulation of the lattice is approximately 0.2 nm. (b) Fourier transform of an (35×35 nm^2) image from a three-layer film. (c) A schematic depiction of the Fourier transform in (b). The numbers are Miller indices (hk) corresponding to the unit cell shown in Fig. 3. The small filled circles correspond to the weak spots at odd values of $h + k$ which would have zero intensity if the unit cell were a perfectly centered rectangle. The open circles correspond to a periodic buckling superstructure which is discussed in Ref. [19]. The scan direction was not rotated relative to the sample as this severely alters the calibration of the AFM; we have, however, imaged many different samples in many orientations relative to the scan direction and the results are perfectly consistent with the unit cell in Fig. 3.

rameters. Inspection of the Fourier transform gives much qualitative information about the lattice symmetry. With the exception of the two spots nearest the origin corresponding to a long-wavelength periodic buckling superstructure [19] [see Fig. 2(c)] the spots in the Fourier transform correspond to a rectangular reciprocal space lattice as shown in Fig. 2(c). This means that the Bravais lattice of the crystal is rectangular as well. However, the spots whose Miller indices (hk) are such that $h+k$ is even are strong while spots corresponding to (hk) such that $h+k$ is odd are weak. In fact, if we ignore the weak (odd $h+k$) spots entirely, the Fourier transform reduces to a pseudohexagonal structure, the special case of a perfectly centered rectangular lattice. However, since the odd spots have a nonvanishing intensity this implies that the two-molecule unit cell is not perfectly centered (see Fig. 3). (The scan direction was not rotated relative to the sample as this severely alters the calibration of the AFM; we have, however, imaged many different samples in many orientations relative to the scan direction and the results are perfectly consistent with the unit cell in Fig. 3.)

The LB films were sufficiently stable to allow enough scanning time to eliminate drift (0.5–2 h, which constitutes hundreds of individual scans), and two images were taken on each of two to five regions (30–40 nm on a side, within 200 nm of each other) on the film surface. Tips that gave images whose Fourier transforms showed fewer than three pairs of distinct spots were discarded. This was true of approximately 15% of the tips tried. The values of $\mathbf{b}_n$ (for the six brightest spots) were averaged for each film; results are plotted as $\theta_{n,n+1}$ vs b_n as shown in Fig. 1. In this representation, the data for a hexagonal lattice, like mica, cluster around a single point on the plot as all three b_n and $\theta_{n,n+1}$ are equal. However, for a (approximately) centered rectangular lattice only two of the three $\mathbf{b}_n$ are equal in magnitude; two of the three angles, $\theta_{n,n+1}$, between adjacent $\mathbf{b}_n$ are equal as well. Each individual data set from each film that showed a lattice (≥ 2 for hydrophobic substrates, ≥ 3 for hydrophilic substrates) appears to be rectangular, and given the error bars determined from measurements of mica, the data sets have identical lattice parameters. Therefore the seven data sets were fit together to obtain the most likely lattice parameters using weights obtained from the uncertainty of the mica measurements. Including uncertainties due to the possible error in calibration, the result of the fit is a noncentered rectangular lattice (with a two-molecule basis) with lengths 0.482 ± 0.004 and 0.748 ± 0.006 nm (see Fig. 3) with the goodness of fit given by $\chi^2\approx 1.1$. This gives a molecular area of 18.0 ± 0.4 Å^2. Measurements on three-layer films of cadmium palmitate (16 carbon chain), stearate (18 carbon chain), and behenate (22 carbon chain) on hydrophilic substrates showed the same lattice (within the quoted error bars). This is in excellent agreement with many measurements of lattice spacings of close-packed, untilted, aliphatic systems [2,3,25] for a particular type of "herringbone" packing, where alternate rows of molecules have an approximately perpendicular orientation with respect to the zig-zag plane of the alkane chain (Fig. 3). Our results for the lattice parameters are also in excellent agreement with recent x-ray diffraction measurements for cadmium arachidate LB films [7].

Except for occasional images which showed grain boundaries between regions of different lattice orientation [19] (this occurred approximately 5% of the time), or dislocations, which typically occurred as bound pairs with opposite Burgers vectors (Fig. 4), the 35×35-nm^2 images showed perfect crystalline order to the limit of our ability to measure it. Figure 5 shows a comparison of a digital Fourier transform of a one-dimensional cross

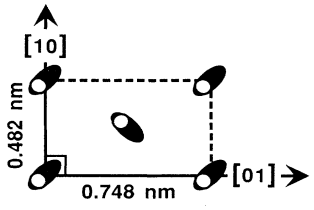

FIG. 3. A schematic diagram of the two-molecule unit cell showing the rectangular lattice explicitly. The ovals represent molecules and the terminal methyl groups are represented by white circles. Dimensions are in nm. The long axis of the oval represents the zig-zag plane of the alkane chain viewed from above. Although we measure only terminal methyl groups, the dimensions that we measure are consistent with this type of "herringbone" structure. Because the molecule in the center has a different orientation than the ones at the vertices of the rectangle, its final methyl group is not centered in the rectangle formed by the final methyl groups of the corner molecules.

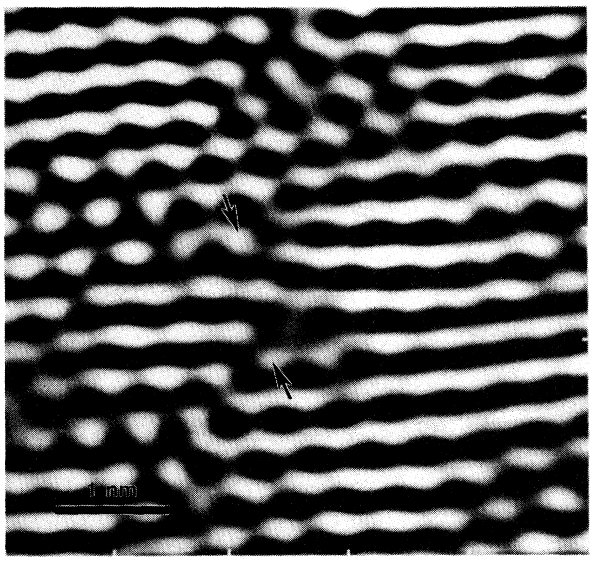

FIG. 4. Portion of an image of a two-layer film on hydrophobic silicon, ~5 nm on a side, showing the presence of a pair of dislocations. This image has been prepared by Fourier transforming the original image and subsequently inverse Fourier transforming only the regions surrounding the three pairs of spots corresponding to the reciprocal lattice vectors. This type of manipulation cannot add defects such as the dislocations shown here. In fact, defects can be masked if too little area surrounding the Fourier spots is selected for the inverse transform.

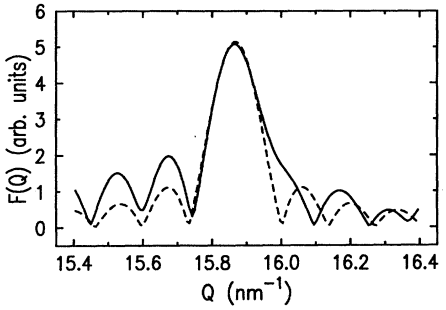

FIG. 5. The solid line is a digital Fourier transform of a cross section, 47 nm long, taken in the (11) direction of a typical lattice image. The dashed line is a Fourier transform of a perfect sine wave, 47 nm in extent. It is apparent that the FWHM's of the two major peaks are approximately equal. This suggests that the lattice has perfect correlations over ≥ 47 nm. The subsidiary maxima and oscillations in the Fourier transform are quite sensitive to the details of the data termination and, therefore, vary substantially from cross section to cross section. However, the essential feature, the FWHM of the peak, depends only on the length of the cross section.

section from a typical lattice image (solid line) with the Fourier transform of a perfect sine wave of wavelength equal to the lattice spacing and arbitrary amplitude (dashed line) over the same distance (47 nm). The subsidiary maxima are due to the abrupt cutoff of the real space data and are quite sensitive to the details of the way the data is terminated. However, the full width at half maximum (FWHM) of the large central peak is independent of the way the data are terminated and is, in fact, indicative of the extent of the correlation of the lattice oscillations. The fact that the FWHM's of the two curves are approximately equal is consistent with the conclusion that the lattice has perfect correlations over lengths ≥ 47 nm. In addition, by imaging several adjacent areas of the film we were able to determine that the orientation of the lattice typically extends at least 200 nm. In fact, it is likely that the size of a grain is greater than 1 μm^2 given the infrequency of our observation of grain boundaries. This is consistent with electron diffraction studies which generally show that the grains extend from micrometers to tens of micrometers [26]. We plan to do more quantitative studies of grain size in the future.

Monolayers of cadmium arachidate deposited on Si and mica were also imaged in air as well as under ethanol using the lowest possible force. In contrast with the multilayers, however, no lattice structure was visible in any monolayer image we have obtained. A smooth, but disordered surface was seen with no features persisting from scan to scan. This implies that the terminal methyl groups are significantly less ordered in a monolayer than in multilayer films [20]. In addition, the monolayer films were more easily damaged by the AFM tip. We could consistently dig a hole through a monolayer by increasing the imaging force above a threshold value of 20 ± 10 nN (the value varied from film to film and from tip to tip). In contrast, we could not damage the multilayer films by increasing the force to the maximum accessible value of ~ 200 nN. A further test was made of the mechanical stability of the films by measuring the time dependence of the water contact angle. Large forces can be present at the contact line due to surface tension [27]. On a monolayer, the initial contact angle of $\sim 95°$ decayed within a few seconds to a value of $\sim 30°$. However, on a three-layer film, the initial contact angle of $99\pm1°$ decayed slowly to a value of $74\pm2°$ over a period of 10 min.

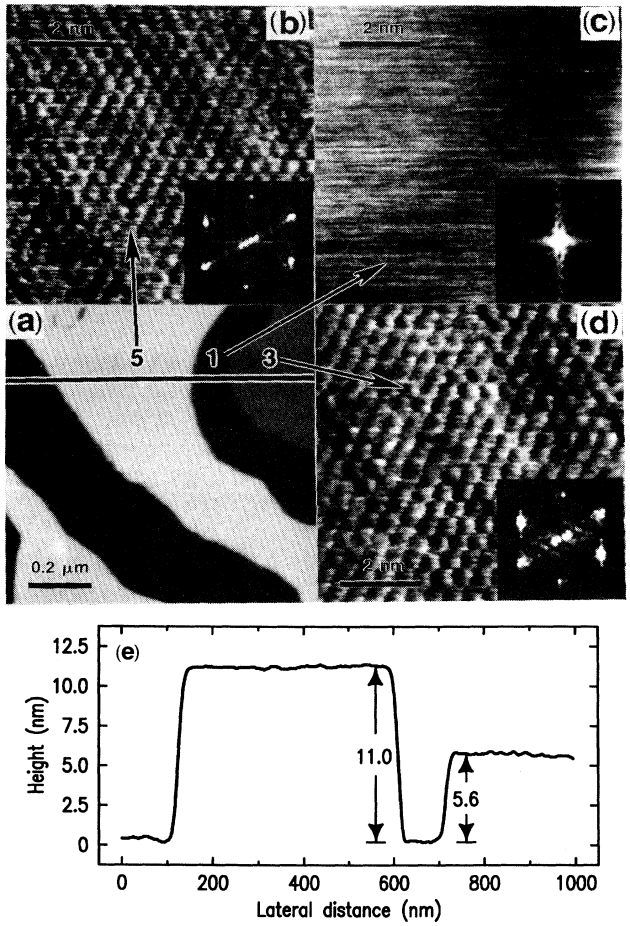

FIG. 6(a) A 1×1-μm^2 image of a nominally three-layer film of cadmium arachidate prepared on a hydrophilic silicon wafer. The film was allowed to rest beneath the subphase for 30 min between the second and third layers, allowing it to reorganize and form regions with different numbers of layers. The image shows regions of different heights separated by steps of 5.6 nm in height, corresponding to bilayer steps. Based on studies [29] of the evolution of the reorganization, we have determined that the domains shown here correspond to thickness of one, three, and five layers, as is shown by the annotation. (b)–(d) show high-resolution images (8×8 nm^2) of the areas marked 1, 3, and 5, respectively. The insets are two-dimensional fast Fourier transforms (FFT) of the respective image. The lattice is clearly visible in the three- and five-layer areas, in both the image and the FFT. No recognizable structure is seen in the one-layer area. (e) shows a cross-sectional plot of height vs distance along the line drawn in (a). The step heights correspond to bilayer steps.

To eliminate any possible effects due to changes in dipping or imaging conditions, we deposited monolayers onto substrates that contained regions with different numbers of cadmium arachidate layers. To do this, we took advantage of the fact that cadmium arachidate films spontaneously reorganize when left under water for periods ≥ 30 min. Thus a nominally two-layer film of cadmium arachidate, if left submerged for 30 min between deposition of the second and third layers, reorganizes to have regions of zero, two, four layers, etc. The size and shape of the domains of differing thickness depend on the length of time the sample is held under water. Upon pulling this substrate through the interface, thereby depositing an additional monolayer, we see regions of one, three, five layers, etc. Hence the outermost monolayer of the film (which is the layer we observe with AFM) was deposited under identical conditions over the entire substrate; the only variation was that different regions of the film had different numbers of cadmium arachidate layers already on the substrate. Figure 6 shows a low magnification image of such a multilayer film as well as representative molecular-resolution images from regions of different thicknesses. Figure 6(a) shows regions of different heights separated by discrete steps of 5.6 nm, which corresponds to the thickness of a bilayer of fully extended cadmium arachidate. Figure 6(e) shows a cross-sectional plot of height versus distance along the line drawn in Fig. 6(a). Based on our observations of the evolution of the reorganization [28], we have determined that the domains shown here correspond to thicknesses

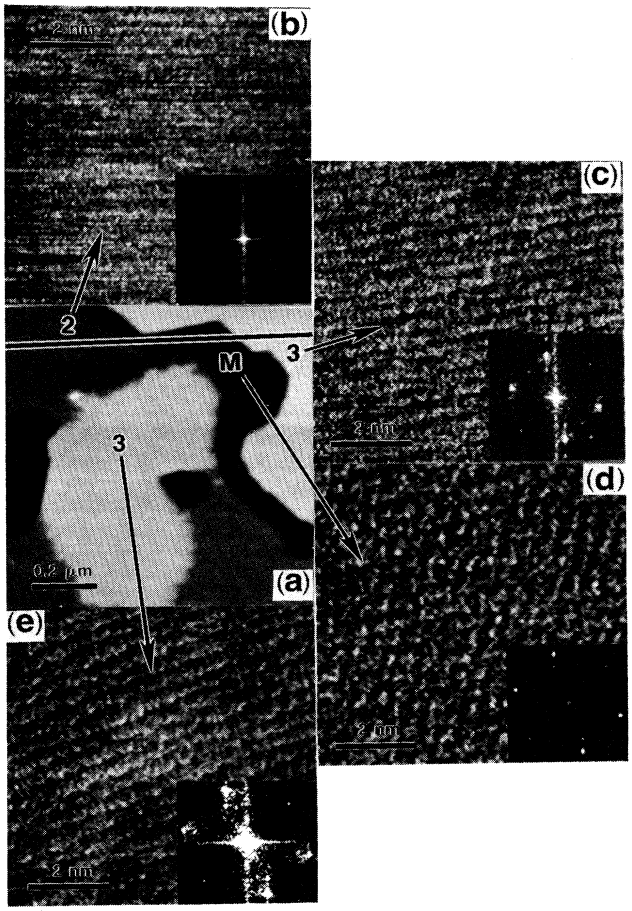

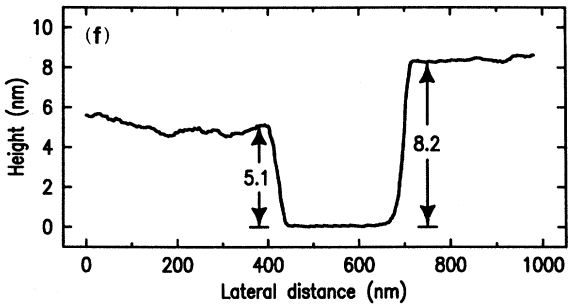

FIG. 7. (a) A 1×1 μm^2 image of a nominally two-layer film of cadmium arachidate prepared on mica and imaged under aqueous subphase. The images were recorded approximately one hour after film deposition. The darkest regions (marked "*M*") correspond to the mica substrate while the other regions correspond to heights of two and three layers as marked. It is likely that the regions marked "3" are actually four layers high; however, the AFM tip pushes through the weakly bound fourth layer to image the sturdy lattice of the third layer below. (b)–(e) show high-resolution images (8×8 nm^2) of the regions marked *M*, 2, and 3, respectively. The insets are two-dimensional fast Fourier transforms of the respective image. A lattice is clearly visible in the regions corresponding to mica and three layers. It is easy to distinguish between the two lattices by quantitative examination of the Fourier transforms. No recognizable structure is seen in the two-layer region. It is generally observed that the resolution of a lattice structure is poorer under water than in air [17], although we do not yet know why. (f) shows a cross-sectional height plot along the line drawn in (a). Although the three-layer region has a height corresponding to ~1.5 times the bulk bilayer repeat distance, the two-layer region is approximately 9% thinner than a crystalline bilayer. This is consistent with its disorder and looser packing.

of one, three, and five layers. Figures 6(b)–6(d) show higher-resolution images (8×8 nm^2) of the areas marked one, three, and five, respectively. The insets are two-dimensional fast Fourier transforms (FFT) of the respective images. The lattice is clearly visible in the three- and five-layer areas, in both the image and the FFT. No recognizable structure is seen in the one-layer area.

The difference in structure between the one-layer areas and the multilayer areas contradicts a long-held belief about LB films, namely, that the structure of the deposited film is simply related to the structure of the monolayer on the water surface [26]. However, the images are consistent with those from homogeneous films; the one-layer region is disordered while the three- and five-layer regions have the rectangular lattice. The results are independent of the total number of layers deposited and also show no variation when mica substrates are used instead of silicon.

By interrupting the deposition process while the film is submerged in the LB trough and transferring the film under aqueous subphase to the AFM, we can measure the reorganization process *in situ*. We have imaged two- and four-layer films on mica and one-layer films on etched, hydrophobic silicon under the aqueous subphase. Figure 7 shows a two-layer film on mica one hour after deposition and higher magnification images of various regions of the film. We see a disordered surface on the regions with a height corresponding to two layers and a lattice on regions with heights corresponding to three layers. We expect that the fourth layer is actually present but not imaged by the AFM. Based on preliminary force measurements, we believe that the AFM tip simply pushes through the weakly bound fourth layer to image the lattice on the tailgroups of the third layer underneath. Analogously, four-layer films on mica under water appear to have regions of three and five layers after reorganization. The four- and six-layer regions are not robust enough to withstand even the smallest forces we can exert with the AFM, $\sim1\times10^{-9}$ N. We can dig a hole in the disordered two-layer region by increasing the imaging force above a threshold value of 20 ± 10 nN; similar to the monolayer in air.

DISCUSSION

Our results highlight a qualitative difference between surface layers that are bound to a layer below a head-group–head-group linkage and those that are not. The surface layer of fatty acids attached to the layers below by a head-group–head-group interface have crystalline order and were mechanically stable regardless of substrate, deposition parameters, number of layers, and im-

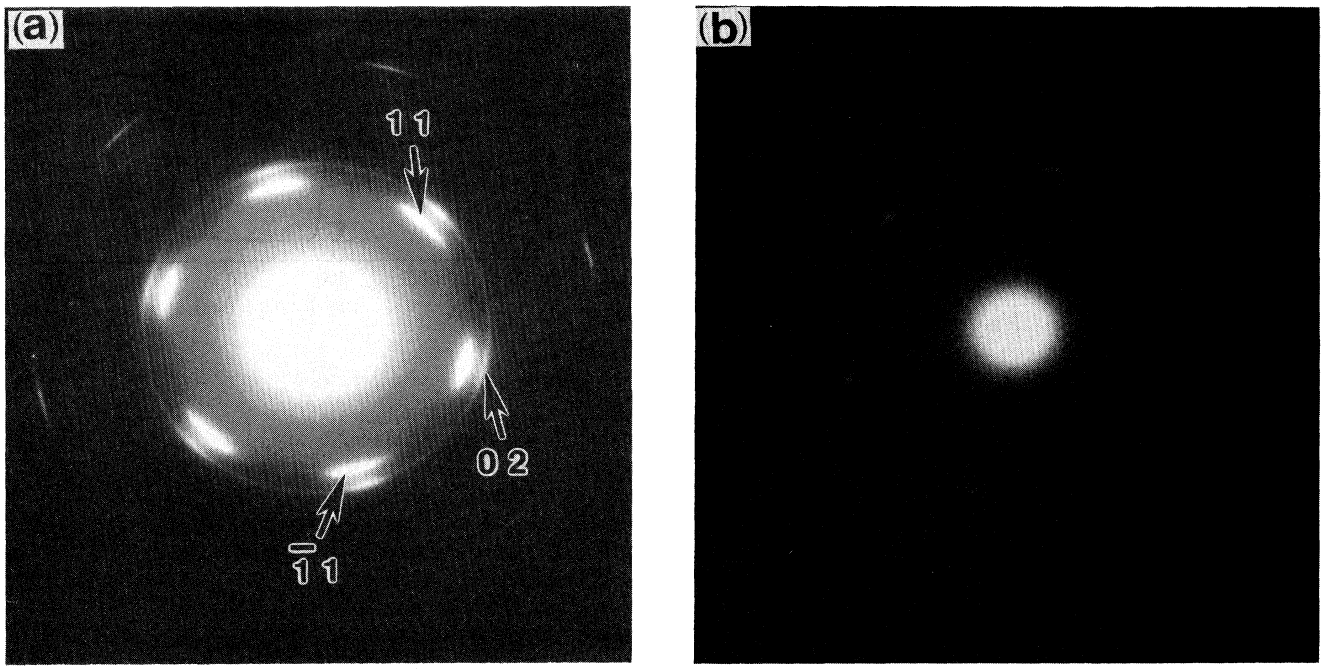

FIG. 8(a) Transmission electron diffraction pattern from a three-layer cadmium arachidate film deposited on a formvar-coated electron microscope grid. Spots from the three twinning directions are visible since the area sampled by the microscope is a circle about 20 μm in diameter, indicating there are at least three distinct grains within the illuminated area. Spots from one particular twinning direction are labeled. Second-order spots are also visible. The large difference between the width of the spots along the radial direction (which is indicative of molecular ordering) and the azimuthal direction (which is indicative of the orientation of the crystalline grains in the films) confirms that the molecular ordering is quite good in comparison to that of the monolayer. Dimensions are given in the text. The weak spots labeled 01 and 10 in Fig. 2(c) are not visible due to the much greater intensity of the 11 and 02 spots. (b) Diffraction pattern from a monolayer of cadmium arachidate. The pattern is hexagonal with dimensions as given in the text. The width of the reflections in the radial direction is much larger in comparison to the width in the azimuthal direction, indicating much less molecular order than in the multilayer (a).

aging conditions. A surface layer attached to the layers below by a tail-group–tail-group interface or a head-group–substrate interface were disordered and much more weakly bound. These weakly bound layers were also much easier to remove with the AFM tip. It is perhaps surprising that the head-group interaction should be so important in determining the order of the entire alkyl chain since the specific lattice structure that we measure is determined by the close packing of the alkane chains. However, we have found that the interaction between head-groups and divalent cations is necessary to stabilize a long-range structure. This finding is supported by electron [3–5] and x-ray [7] diffraction results which show the translational correlation length in monolayers to be between 30 Å and 100 Å, significantly less than the ≥ 470 Å we have seen on the thicker films. The importance of the head-group–head-group interface may explain the well-known empirical result that LB films of fatty acid salts (with divalent cations) are more stable [13] and easier to make [29] than LB films of the analogous fatty acid. It is also likely that the strong head-group interaction is the energetic driving force of the reorganization under water.

To confirm our AFM studies, we performed electron diffraction on one- and three-layer films on a hydrophilic substrate. The diffraction pattern from the three-layer film [Fig. 8(a)] agrees quantitatively with our AFM results. The diffraction pattern from the three-layer films shows sharp reflections, higher-order reflections, and evidence of twinning, indicative of long-range order, as do the AFM images. This is evident in the large difference between the width of the spots along the radial direction (which is indicative of molecular ordering) and the azimuthal direction (which is indicative of the orientation of the crystalline grains in the films). The diffraction from the monolayer, however [Fig. 8(b)], agrees with other electron and x-ray diffraction data [2–4,7] and shows a hexagonal structure with a nearest-neighbor distance of 0.47 ± 0.01 nm, giving an area per molecule of 19.4 $Å^2$, about 8% larger than in multilayer films. The monolayer reflections are almost as wide in the radial direction as in the azimuthal direction, indicating much less molecular order in the monolayer. The extra area per molecule of the monolayer film and the short-range positional correlation length [3–5,7] implies that there is considerable motion and disorder within the individual alkane chains as compared to the close-packed chains in the multilayer (area per molecule of 18 $Å^2$). This is supported by FTIR spectroscopy measurements [2,16] which show that the alkane chains of monolayers show less crystallinity than in thicker films. This increased disorder in the alkane chains of monolayers is consistent with our AFM images that show an absence of order at the methyl end of the chains.

CONCLUSION

We have obtained molecular-resolution images and high-resolution Fourier transforms of LB films of fatty acids over areas of ≥ 1200 nm^2 [19,20]. This area is limited by the ability of the instrument to resolve objects less than about 1/100 of a scan dimension (only 400 samples are taken per line). In combination with careful calibration and evaluation of errors, we can determine the lattice symmetry with good precision. This ability is a necessary first step to any experimental work on two-dimensional lattices. Given the quality and size of the lattice images, we can make quantitative measurements of lattice defects, such as dislocation density and average distance between members of dislocation pairs. Such measurements are essential to test theories of two-dimensional melting transitions [17–20], only AFM imaging is capable of this type of resolution.

The AFM images show that the essential factor in determining order and stability *in the alkyl chains* in cadmium arachidate films is the presence of an adjacent head-group–head-group interface stabilized by cadmium ions. The role of the interface (substrate or free surface) in determining molecular ordering is only to allow or disallow the adjacent head-group–head-group stabilization. The structure and phase of the monolayer on the subphase are also not simply related to the structure and phase of the deposited Langmuir-Blodgett film; strong coupling effects to other layers have an equal or greater effect on determining the structure of the deposited films.

ACKNOWLEDGMENTS

This work was supported by the Office of Naval Research under Grant No. N00014-90-J-1551, the National Science Foundation under Grant No. CTS90-15537, the National Institutes of Health under Grant No. GM 47334, and the Donors of the Petroleum Research Foundation. We acknowledge J. Israelachvili, W. Ducker, and S. Steinberg for useful discussions. We also thank Frank Grunfeld of NIMA Technologies for his assistance with the trough and software.

[1] G. G. Roberts, Adv. Phys. **34**, 475 (1985).
[2] A. Bonnerot, P. A. Chollet, H. Frisby, and M. Hoclet, J. Chem. Phys. **97**, 365 (1985).
[3] S. Garoff, H. W. Deckman, J. H. Dunsmuir, and M. S. Alvarez, J. Phys. (Paris) **47**, 701 (1986).
[4] C. Böhm, R. Seitz, and H. Riegler, Thin Solid Films **178**, 511 (1989).
[5] I. R. Peterson, R. Seitz, H. Krug, and I. Voigt-Martin, J. Phys. (Paris) **51**, 1003 (1990).
[6] M. Seul, P. Eisenberger, and H. M. McConnell, Proc. Natl. Acad. Sci. USA **80**, 5795 (1983); M. Prakash, P. Dutta, J. B. Ketterson, and B. M. Abraham, Chem. Phys. Lett. **111**, 395 (1984).
[7] P. Tippmann-Krayer, R. M. Kenn, and H. Möhwald, Thin Solid Films **210**, 577 (1992).
[8] M. Pomerantz and A. Segmüller, Thin Solid Films **68**, 33 (1980).
[9] R. F. Fischetti, V. Skita, A. F. Garito, and J. K. Blasie, Phys. Rev. B **37**, 4788 (1988); S. Xu, A. Murphy, S. M. Amador, and J. K. Blasie, J. Phys. (Paris) I **1**, 1131 (1991).

[10] V. Skita, W. Richardson, M. Filiplowski, A. Garito, and J. K. Blasie, J. Phys. **47**, 1849 (1986); V. Skita, M. Filipkowski, A. F. Garito, and J. K. Blasie, Phys. Rev. B **34**, 5826 (1986).

[11] J. M. Bloch, W. B. Yun, and K. M. Mohanty, Phys. Rev. B **40**, 6529 (1989).

[12] D. A. Outka, J. Stöhr, J. P. Rabe, J. D. Swalen, and H. H. Rotermund, Phys. Rev. Lett. **59**, 1321 (1987).

[13] P. M. Claesson and J. M. Berg, Thin Solid Films **176**, 157 (1989).

[14] L. Rothberg, G. S. Higashi, D. L. Allara, and S. Garoff, Chem. Phys. Lett. **133**, 67 (1987); J. P. Rabe, J. D. Swalen, and J. F. Rabolt, J. Chem. Phys. **86**, 1601 (1987); T. Nakanaga, M. Matsumoto, Y. Kawabata, H. Takeo, and C. Matsamura, Chem. Phys. Lett. **160**, 129 (1989).

[15] P. Stroeve, M. P. Srinivasan, B. G. Higgins, and S. T. Kowel, Thin Solid Films **146**, 209 (1987).

[16] R. Maoz and J. Sagiv, J. Colloid Interface Sci. **100**, 465 (1984); F. Kimura, J. Umemura, and T. Takenaka, **2**, 96 (1986); M. Shimomura, K. Song, and J. F. Rabolt, *ibid.* **8**, 887 (1992).

[17] M. Egger, F. Ohnesorge, A. L. Weisenhorn, S. P. Heyn, B. Drake, C. B. Prater, S. A. C. Gould, P. K. Hansma, and H. E. Gaub, J. Struct. Biol. **103**, 89 (1990); E. Meyer, L. Howald, R. M. Overney, H. Heinzelmann, J. Frommer, H.-J. Güntherodt, T. Wagner, H. Schier, and S. Roth, Nature (London) **349**, 398 (1991); J. A. N. Zasadzinski, C. A. Helm, M. L. Longo, A. L. Weisenhorn, S. A. C. Gould, and P. K. Hansma, Biophys. J. **59**, 755 (1991); L. Bourdieu, P. Silberzan, and D. Chatenay, Phys. Rev. Lett. **67**, 2029 (1991).

[18] D. P. E. Smith, A. Bryant, C. F. Quate, J. P. Rabe, Ch. Gerber, J. D. Swalen, Proc. Natl. Acad. Sci. USA **84**, 969 (1987); J. P. Rabe and S. Buchholz, Phys. Rev. Lett. **66**, 2096 (1991); J. K. H. Hörber, C. A. Lang, T. W. Hänsch, W. M. Heckl, and H. Möhwald, Chem. Phys. Lett. **145**, 151 (1988).

[19] J. Garnaes, D. K. Schwartz, R. Viswanathan, and J. A. N. Zasadzinski, Nature (London) **357**, 54 (1992); H. G. Hansma, S. A. C. Gould, P. K. Hansma, H. E. Gaub, M. L. Longo, and J. A. N. Zasadzinski, Langmuir **7**, 1051 (1991); R. Viswanathan, D. K. Schwartz, J. Garnaes, and J. A. N. Zasadzinski, *ibid.* **8**, 1603 (1992).

[20] D. K. Schwartz, J. Garnaes, R. Viswanathan, and J. A. N. Zasadzinski, Science **257**, 508 (1992).

[21] Millipore Corp., Bedford, MA.

[22] NIMA Technology Ltd., Warwick Science Park, Coventry, CV4 7EZ, England.

[23] Silicon wafers polished on both sides [orientation (100), 3–5 Ω cm, *n* type, ~0.4 mm thick] with a rms roughness of approximately 2 Å as measured by AFM. Semiconductor Processing, Boston, MA.

[24] Nanoscope II FM, Digital Instruments, Inc. Goleta, CA 93117.

[25] A. I. Kitaigorodskii, *Organic Chemical Crystallography* (Consultant Bureau, New York, 1961); F. Leveiller, D. Jacquemain, M. Lahav, L. Leiserowitz, M. Deutsch, K. Kjaer, J. Als-Nielsen, Science **252**, 1532 (1991); M. L. Schlossman, D. K. Schwartz, P. S. Pershan, E. H. Kawamoto, G. J. Kellogg, and S. Lee, Phys. Rev. Lett. **66**, 1599 (1991).

[26] R. Steitz, E. E. Mitchell, and I. R. Peterson, Thin Solid Films **205**, 124 (1991).

[27] J. N. Israelachvili, *Intermolecular and Surface Forces,* 2nd ed. (Academic, London, 1992), Chap. 15.

[28] D. K. Schwartz, V. Viswanathan, and J. A. N. Zasadzinski, J. Phys. Chem. (to be published).

[29] E. P. Honig, J. H. Th. Hengst, and D. den Engelsen, J. Colloid Interface Sci. **45**, 92 (1973).

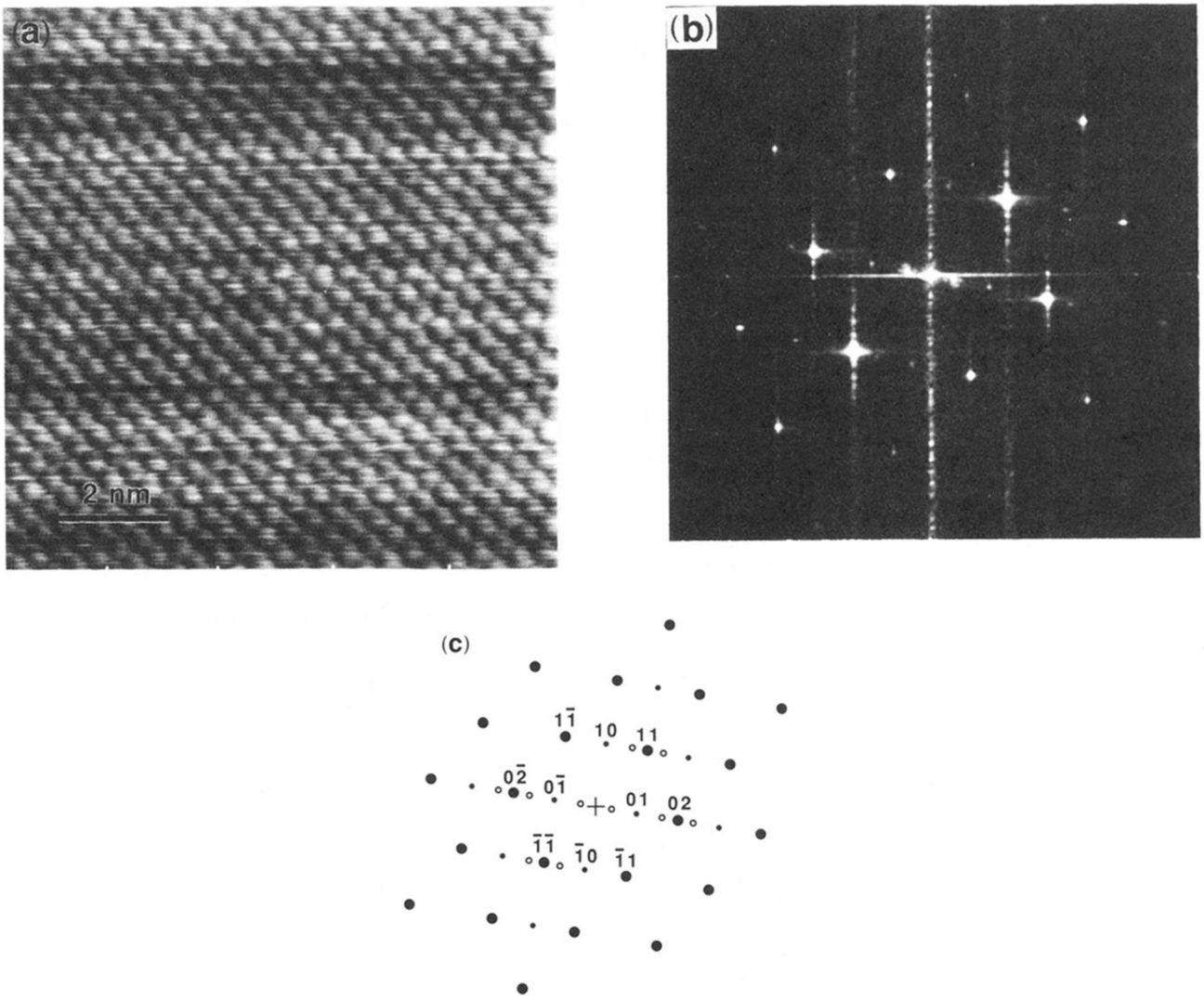

FIG. 2. (a) Raw image of a four-layer LB film of cadmium arachidate on hydrophobic silicon (10×10 nm^2). The images used for analysis were typically 35 nm on a side; however, the molecular details are easier to see in a portion cut from these images. The peak to valley height modulation of the lattice is approximately 0.2 nm. (b) Fourier transform of an (35×35 nm^2) image from a three-layer film. (c) A schematic depiction of the Fourier transform in (b). The numbers are Miller indices (hk) corresponding to the unit cell shown in Fig. 3. The small filled circles correspond to the weak spots at odd values of $h+k$ which would have zero intensity if the unit cell were a perfectly centered rectangle. The open circles correspond to a periodic buckling superstructure which is discussed in Ref. [19]. The scan direction was not rotated relative to the sample as this severely alters the calibration of the AFM; we have, however, imaged many different samples in many orientations relative to the scan direction and the results are perfectly consistent with the unit cell in Fig. 3.

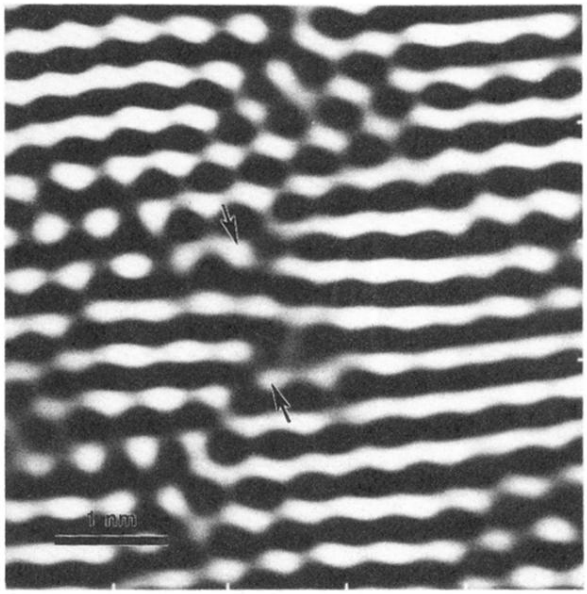

FIG. 4. Portion of an image of a two-layer film on hydrophobic silicon, ~5 nm on a side, showing the presence of a pair of dislocations. This image has been prepared by Fourier transforming the original image and subsequently inverse Fourier transforming only the regions surrounding the three pairs of spots corresponding to the reciprocal lattice vectors. This type of manipulation cannot add defects such as the dislocations shown here. In fact, defects can be masked if too little area surrounding the Fourier spots is selected for the inverse transform.

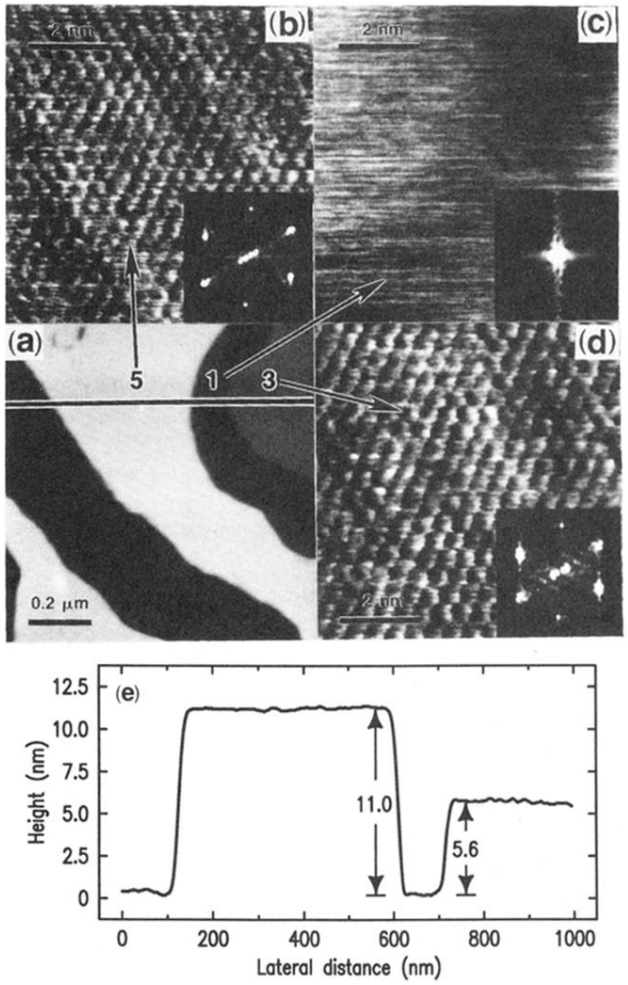

FIG. 6(a) A 1×1-μm^2 image of a nominally three-layer film of cadmium arachidate prepared on a hydrophilic silicon wafer. The film was allowed to rest beneath the subphase for 30 min between the second and third layers, allowing it to reorganize and form regions with different numbers of layers. The image shows regions of different heights separated by steps of 5.6 nm in height, corresponding to bilayer steps. Based on studies [29] of the evolution of the reorganization, we have determined that the domains shown here correspond to thickness of one, three, and five layers, as is shown by the annotation. (b)–(d) show high-resolution images (8×8 nm^2) of the areas marked 1, 3, and 5, respectively. The insets are two-dimensional fast Fourier transforms (FFT) of the respective image. The lattice is clearly visible in the three- and five-layer areas, in both the image and the FFT. No recognizable structure is seen in the one-layer area. (e) shows a cross-sectional plot of height vs distance along the line drawn in (a). The step heights correspond to bilayer steps.

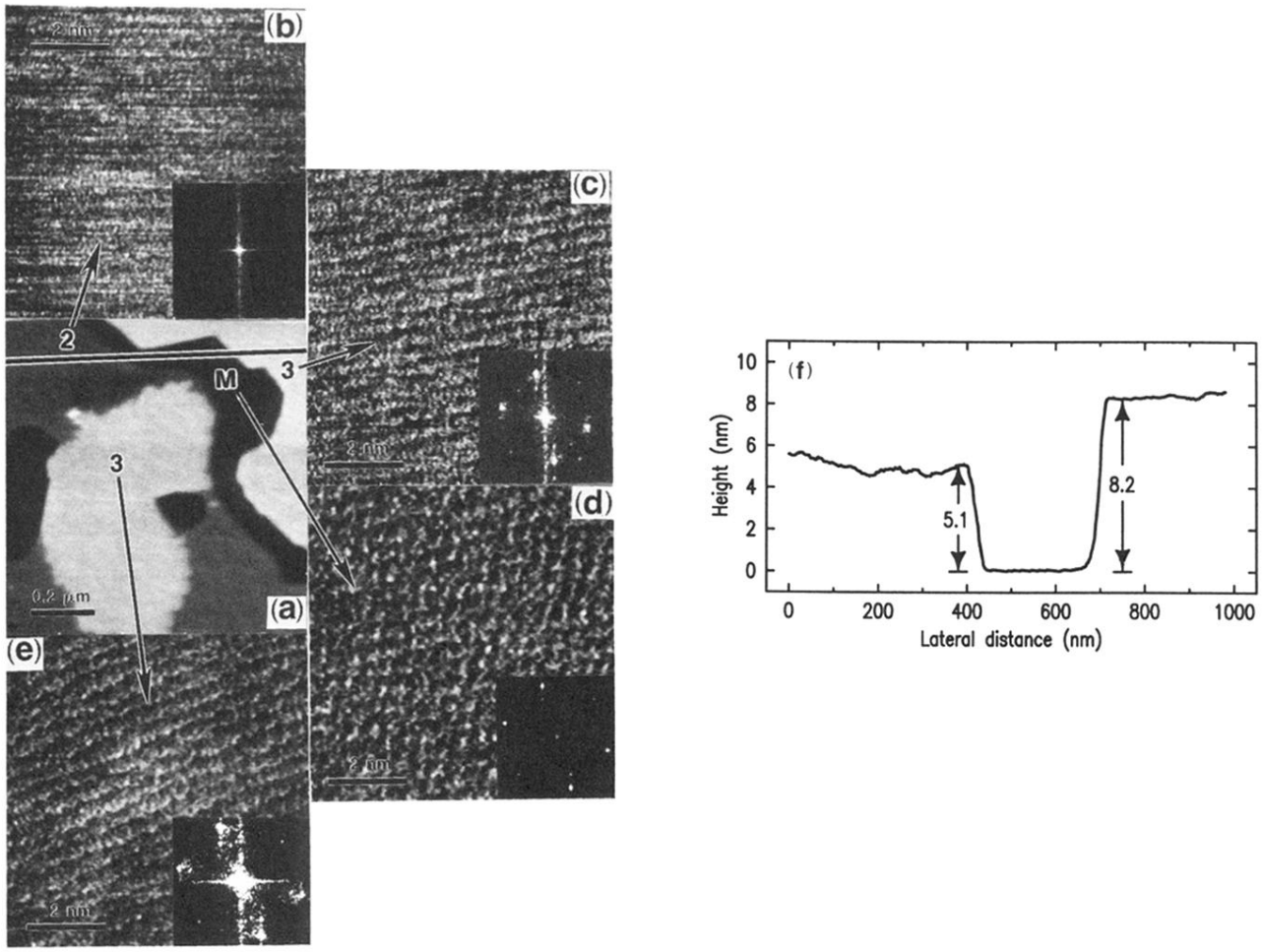

FIG. 7. (a) A 1×1 μm^2 image of a nominally two-layer film of cadmium arachidate prepared on mica and imaged under aqueous subphase. The images were recorded approximately one hour after film deposition. The darkest regions (marked "*M*") correspond to the mica substrate while the other regions correspond to heights of two and three layers as marked. It is likely that the regions marked "3" are actually four layers high; however, the AFM tip pushes through the weakly bound fourth layer to image the sturdy lattice of the third layer below. (b)–(e) show high-resolution images (8×8 nm^2) of the regions marked *M*, 2, and 3, respectively. The insets are two-dimensional fast Fourier transforms of the respective image. A lattice is clearly visible in the regions corresponding to mica and three layers. It is easy to distinguish between the two lattices by quantitative examination of the Fourier transforms. No recognizable structure is seen in the two-layer region. It is generally observed that the resolution of a lattice structure is poorer under water than in air [17], although we do not yet know why. (f) shows a cross-sectional height plot along the line drawn in (a). Although the three-layer region has a height corresponding to ~1.5 times the bulk bilayer repeat distance, the two-layer region is approximately 9% thinner than a crystalline bilayer. This is consistent with its disorder and looser packing.

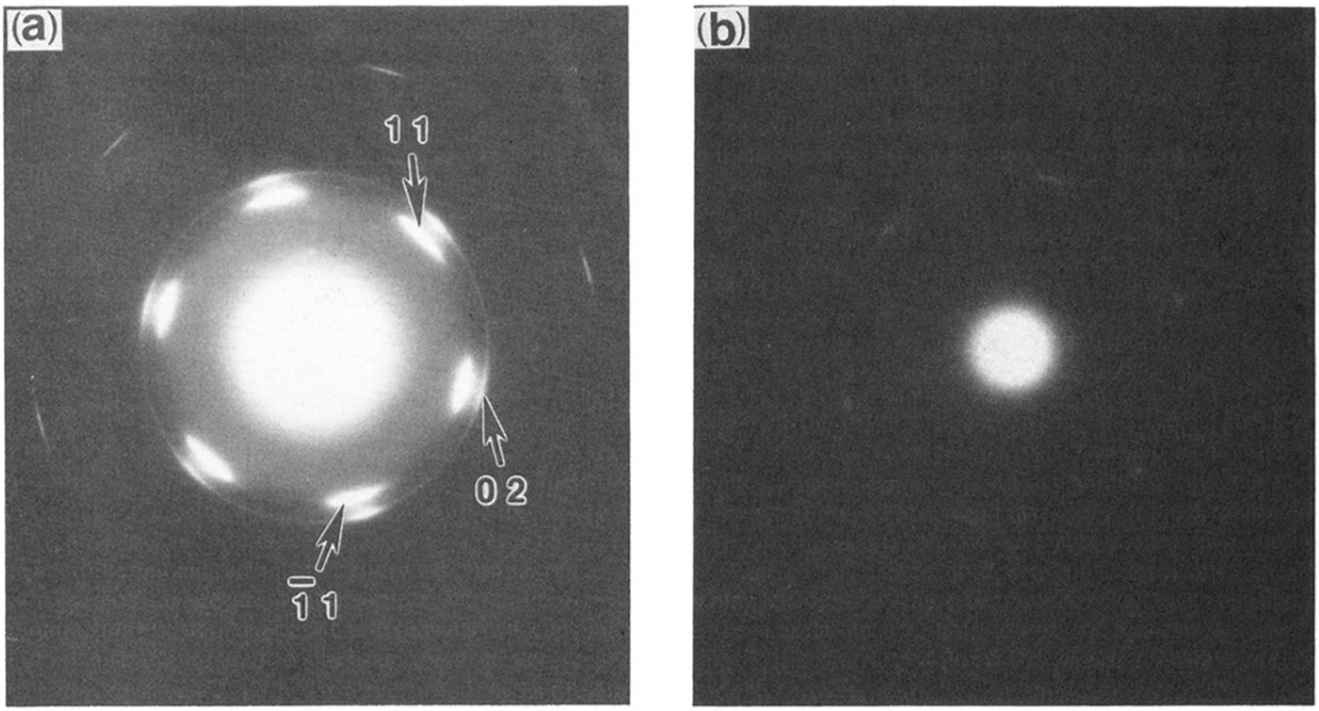

FIG. 8(a) Transmission electron diffraction pattern from a three-layer cadmium arachidate film deposited on a formvar-coated electron microscope grid. Spots from the three twinning directions are visible since the area sampled by the microscope is a circle about 20 μm in diameter, indicating there are at least three distinct grains within the illuminated area. Spots from one particular twinning direction are labeled. Second-order spots are also visible. The large difference between the width of the spots along the radial direction (which is indicative of molecular ordering) and the azimuthal direction (which is indicative of the orientation of the crystalline grains in the films) confirms that the molecular ordering is quite good in comparison to that of the monolayer. Dimensions are given in the text. The weak spots labeled 01 and 10 in Fig. 2(c) are not visible due to the much greater intensity of the 11 and 02 spots. (b) Diffraction pattern from a monolayer of cadmium arachidate. The pattern is hexagonal with dimensions as given in the text. The width of the reflections in the radial direction is much larger in comparison to the width in the azimuthal direction, indicating much less molecular order than in the multilayer (a).